Galaxies in 3D across the Universe
Proceedings IAU Symposium No. 309, 2014
B. L. Ziegler, F. Combes, H. Dannerbauer, M. Verdugo, eds.

doi:10.1017/S1743921314009399

The star formation history of galaxies in 3D: CALIFA perspective

R. M. González Delgado[1], R. Cid Fernandes[2], R. García-Benito[1], E. Pérez[1], A. L. de Amorim[2], C. Cortijo-Ferrero[1], E. A. D. Lacerda[2], R. López Fernández[1], S. F. Sánchez[1,3], N. Vale Asari[2] and CALIFA collaboration

[1]Instituto de Astrofísica de Andalucía (CSIC), Glorieta de la Astronomía s/n, E-18008 Granada, Spain
email: rosa@iaa.es
[2]Departamento de Física, Universidade Federal de Santa Catarina, P. O. Box 476, 88040-900, Florianópolis, SC, Brazil
[3]Instituto de Astronomía,Universidad Nacional Autonóma de Mexico, A. P. 70-264, 04510, México,D. F.

Abstract. We resolve spatially the star formation history of 300 nearby galaxies from the CALIFA integral field survey to investigate: a) the radial structure and gradients of the present stellar populations properties as a function of the Hubble type; and b) the role that plays the galaxy stellar mass and stellar mass surface density in governing the star formation history and metallicity enrichment of spheroids and the disks of galaxies. We apply the fossil record method based on spectral synthesis techniques to recover spatially and temporally resolved maps of stellar population properties of spheroids and spirals with galaxy mass from 10^9 to $7{\times}10^{11}$ $M_\odot$. The individual radial profiles of the stellar mass surface density ($\mu_\star$), stellar extinction (A_V), luminosity weighted ages ($\langle \log age \rangle_L$), and mass weighted metallicity ($\langle \log Z/Z_\odot \rangle_M$) are stacked in seven bins of galaxy morphology (E, S0, Sa, Sb, Sbc, Sc and Sd). All these properties show negative gradients as a sight of the inside-out growth of massive galaxies. However, the gradients depend on the Hubble type in different ways. For the same galaxy mass, E and S0 galaxies show the largest inner gradients in $\mu_\star$; and Andromeda-like galaxies (Sb with log $M_\star(M_\odot) \sim 11$) show the largest inner age and metallicity gradients. In average, spiral galaxies have a stellar metallicity gradient $\sim$ -0.1 dex per half-light radius, in agreement with the value estimated for the ionized gas oxygen abundance gradient by CALIFA. A global ($M_\star$-driven) and local ($\mu_\star$-driven) stellar metallicity relation are derived. We find that in disks, the stellar mass surface density regulates the stellar metallicity; in spheroids, the galaxy stellar mass dominates the physics of star formation and chemical enrichment.

Keywords. galaxies: evolution – galaxies: formation – galaxies: fundamental parameters – galaxies: stellar content – galaxies: structure

1. Introduction

Much of we know about galaxy properties has come from panoramic imaging or 1D spectroscopic surveys. While imaging provides useful 2D information of galaxy morphology and structural properties, spectroscopic surveys give information on the central or global stellar population and ionized gas properties and kinematics. However, galaxies are a complex mix of stars, interstellar gas, dust and dark matter, distributed in their disks and bulges, and resolved spatial information is needed to constrain the formation processes and evolution of the galaxy sub-components.

Integral Field Spectroscopy (IFS) observations can provide a unique 3D view of galaxies (two spacial plus one spectral dimensions), and allows to recover 2D maps of the stellar

population and ionized gas properties, and kinematics. Until very recently it was not possible to obtain IFS data for sample larger than a few tens of galaxies. ALTAS3D (Cappellari *et al.* 2011), CALIFA (Sánchez *et al.* 2012), SAMI (Croom *et al.* 2012) and MaNGA (Bundy *et al.* 2014) surveys are the first in doing this steep forward, taking observations of several hundreds to several thousands of galaxies of the nearby Universe.

CALIFA is our currently-ongoing survey, observing 600 nearby galaxies with the PPaK IFU at the 3.5m telescope of Calar Alto observatory. The observations cover 3700-7000 Å with an intermediate spectral resolution (fwhm $\sim$ 6 Å in the data presented in this contribution) and $\sim$1arcmin^2 field of view with a final spatial sampling of 1 arcsec. Galaxies were selected from SDSS in the redshift range $0.005 \leqslant z \leqslant 0.03$, covering all the color magnitude diagram down to $M_r \leqslant$ -18, resulting in a sample containing all morphological types. An extended description of the survey, data reduction and sample can be found in Sánchez *et al.*(2012), Hussemann *et al.*(2012) and Walcher *et al.*(2014).

Previously, we derived the spatial resolved star formation history of the CALIFA galaxies on the first data release (DR1) using the fossil records that the stellar populations imprint in the galaxy spectra. This method dissects galaxies in space and time providing a 3D information that allows to retrieve when and where the mass and stellar metallicity were assembled as a function of look-back-time. We use the *STARLIGHT* code (Cid Fernandes *et al.*2005) to do a λ-by-λ spectral fit using different sets of single stellar population (SSP) models. These SSP are from a combination of Vazdekis *et al.* (2010) and Gonzáles Delgado *et al.*(2005) (labelled GMe), or from Charlot & Bruzual (2007) (labelled CBe).

Our scientific results from the first 100 CALIFA galaxies were presented in Pérez *et al.*(2013), Cid Fernandes *et al.*(2013, 2014) and Gonzáles Delgado *et al.*(2014a). One highlight result of these works is that the signal of downsizing is spatially preserved, with inner and outer regions growing faster for more massive galaxies, consequence of the inside-out growth of massive galaxies.

Here, based on the fossil records analysis of 300 CALIFA galaxies we present the results on: a) the radial structure and gradients of the stellar populations as a function of the Hubble type; and b) the role that plays the galaxy mass and stellar mass surface density in governing the star formation history and metallicity enrichment in ellipticals and in the bulge and disk components of galaxies.

Two complementary contributions to this one are presented in these proceedings: Sánchez presents CALIFA survey in the context of other contemporaneous IFS surveys such as SAMI and MaNGA; and Cid Fernandes *et al.* explains in details the methodology that we apply here, the uncertainties associated to the method, and results related with the growth of mass and metallicity in galaxies and their evolution.

2. Results

We present new results based on the radial structure of the present stellar population properties of 300 CALIFA galaxies that were observed with the V500 and V1200 setups and calibrated with the new pipeline 1.4 (see García-Benito *et al.* 2014 for details). 1D spatial radial profiles are obtained from the 2D maps, with an azimuthal averaging by an elliptical xy-to-R conversion. These 2D maps are created after collapsing the SFH in the time domain. The results are presented by stacking each galaxy individual radial profiles that has been previously normalized to a common metric that uses the half-light-radius (HLR) of each galaxy.

2.1. *Hubble sequence: stellar population properties of galaxies in the tuning-fork diagram*

One step to understand how galaxies form and evolve is classifying galaxies and studying their properties. Most of the massive galaxies in the near Universe are E, S0 and spirals (Blanton & Moustakas 2009), following well the Hubble tuning-fork diagram. The bulge fraction seems to be one of the main physical parameters that produce the Hubble sequence, increasing from late to early spirals. In this scheme, S0 galaxies are a transition class between the spiral classes and the elliptical one, with large bulges, but intermediate between Sa and E galaxies. On the other hand, galaxies properties such as color, mass, surface brightness, luminosity, and gas fraction are correlated with the Hubble type (Robert & Haynes 1994). This suggests that the Hubble sequence can illustrate possible paths for galaxy formation and evolution. If so, how is the spatial resolved stellar population properties of galaxies correlated with the Hubble type? Can the Hubble-tuning-fork scheme be useful to organize galaxies per galaxy mass and age or galaxy mass and metallicity?

CALIFA is a suitable benchmark to address these questions because it includes a significant amount of E, S0 and spirals. After a visual classification, the 300 galaxies were grouped in 41 E, 32 S0, 51 Sa, 53 Sb, 58 Sbc, 50 Sc, and 15 Sd. This sub-sample is a well representation of the morphological distribution of the whole CALIFA sample. Here we present the radial structure of the stellar mass surface density ($\mu_\star$), stellar extinction (A_V), luminosity weighted stellar age ($\langle \log age \rangle_L$), mass weighted stellar metallicity ($\langle \log Z/Z_\odot \rangle_M$), by stacking the galaxies by their Hubble type. First, we present how galaxies are distributed by stellar mass ($M_\star$) and their sizes in mass (a_{50}^M: radius that contains half of the mass) and in light (a_{50}^L: radius that contains half of the light, HLR). Most of the results discussed here are obtained with the *GMe* SSP models, but similar results are obtained with the *CBe* base (see Fig.1).

Galaxy stellar mass: We obtain the galaxy stellar mass ($M_\star$) after resolving spatially the SFH of each zone and hence, taking into account spatial variation of the stellar extinction and M/L ratio. Fig.1a shows the distribution of $M_\star$ as a function of Hubble type. The mass ranges from 10^9 to $7{\times}10^{11}$ $M_\odot$ (*GMe*). We see a clear segregation in mass: galaxies with high bulge -to-disk ratio (E, S0, Sa) are the most massive ones ($\geqslant 10^{11}$ $M_\odot$), and galaxies with small bulges (Sc-Sd) have masses $M \leqslant 10^{10}$ $M_\odot$. The galaxy stellar mass distribution obtained with *CBe* models is similar to $M_\star$ with *GMe* base, but shifted by -0.25 dex due to the change of IMF (Chabrier with *GMe* and Salpeter with *GMe* SSP models)

Galaxy size: We take the advantage of our spatially resolved SFH and extinction maps to show that galaxies are more compact in mass than in light (González Delgado *et al.* 2014a), resulting in a ratio of the radius that contains half of mass with respecto to the ratio that contains half of the light (a_{50}^M/a_{50}^L) of 0.8. Galaxies are therefore typically 20% smaller in mass than how they appear in optical light. Fig.1b shows the distribution of a_{50}^M/a_{50}^L as a function of Hubble type, and a clear trend is observed. Sa-Sb-Sbc have the lowest a_{50}^M/a_{50}^L, due to the fact that they show a very prominent old bulge which have similar central properties to the spheroidal components of S0 and E, but a blue and extended disc which contributes to the light in the range Sa to Sbc.

Stellar mass surface density: The left panel in Fig.2 shows the radial profiles (in units of a_{50}^L) of log $\mu_\star$ obtained with *GMe* SSP base. Individual results are stacked in seven morphological bins. Error bars in the panel indicate the dispersion at one a_{50}^L distance in the galaxies of the Sa class, but it is similar for other Hubble type and radial distance. Negative gradients are detected in all galaxy types and increase from late type

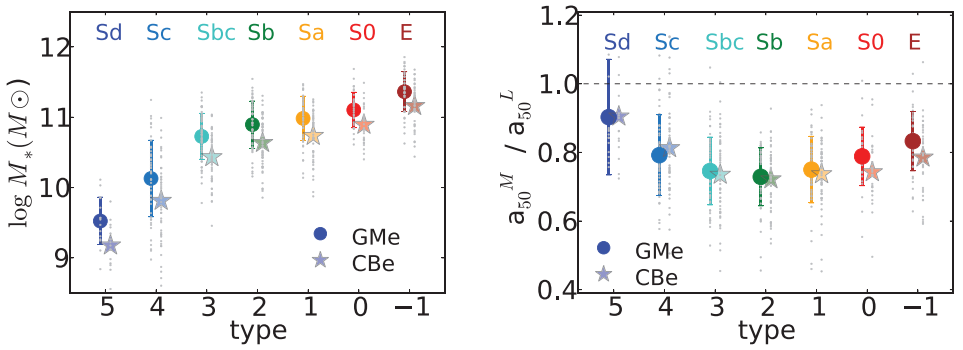

Figure 1. Left: Distribution of the galaxy stellar masses obtained from the spatially resolved spectral fits of each galaxy for each Hubble type of the galaxy of this work (grey small points). The coloured dots and stars are the mean galaxy stellar mass in each Hubble type obtained with the GMe and CBe SSP models. The bars show the dispersion in mass. Right: Relation between a_{50}^M/a_{50}^L and Hubble type. Symbols are as in the left panel of the figure.

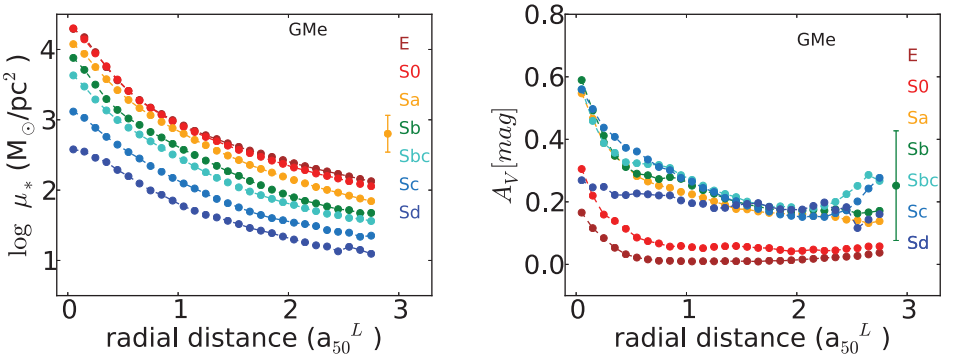

Figure 2. Radial profiles of the stellar mass surface density (in logarithm scale, log $\mu_\star$) and the stellar extinction A_V as a function of Hubble type. The radial distance is in HLR units.

(Sd) to early type (S0, and E) galaxies. At a constant $M_\star$, spheroidal (S0 and E) are more compact than spirals, and S0 and E galaxies have similar compactness at all distances.

Stellar extinction: The right panel in Fig.2 shows the radial profiles A_V. All galaxy types show radial profiles that increase toward the center. Early type galaxies (E, and S0) are also extinguished toward the nucleus by 0.2-0.4 mag, while out of 1 HLR of the galaxies, the (old) stellar population are almost reddening-free. All spiral disks show ∼0.2-0.3 mag extinction. The bulges are significantly more extinguished up to 0.6 mag, except the bulges of late type spirals (Sd) that A_V is similar to the extinction in the disk.

Stellar ages: The left panel of Fig.3 shows the radial profiles of $\langle \log age \rangle_L$ (in yr). Symbols are as in Fig.2. Negative gradients are detected for all the Hubble types, suggesting that the quenching is progressing outwards, and the galaxies are growing inside-out, as we concluded with our mass assembly growth analysis (Pérez *et al.* 2012). Inner gradients are calculated between the galaxy nucleus and at 1 a_{50}^L, and the outer gradient between 1 and 2 a_{50}^L. The inner age gradient shows a clear behaviour with Hubble type, being maximum for spirals of intermediate type (Sb-Sbc). At $M_\star$ constant, Sb-Sbc galaxies have the largest age gradient. The age gradient in the outer disk (between 1 and 2 a_{50}^L) is smaller than the inner ones, but again it is larger for the spiral Sa-Sb-Sbc.

Stellar metallicity: The right panel in Fig.3 shows the radial profiles of mass weighted stellar metallicity obtained as explained in González Delgado *et al.*(2014b). Except for

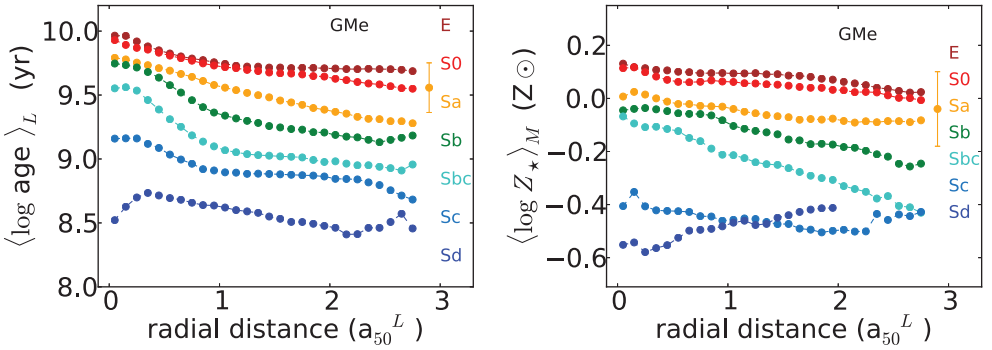

Figure 3. As in Fig.2 for the luminosity weighted ages and the mass weighted metallicity.

late spirals (Sc-Sd), spirals present negative gradients in average $\sim$ -0.1dex per HLR, similar to the value obtained for the nebular oxygen abundances obtained by CALIFA (Sánchez *et al.* 2013). For galaxies of equal stellar mass, the intermediate type spirals (Sbc) have the largest gradients. These negative gradients again are sights of the inside-out growth of the disks. However, the metallicity gradient for late spirals is positive indicating that these galaxies, in the low mass galaxy bins, may be formed from outside-in. This result is also in agreement with our results from the mass assembly evolution (Pérez *et al.* 2012).

2.2. *The role of $\mu_\star$ and $M_\star$ in the SFH and chemical enrichment of galaxies*

The galaxy stellar mass is also considered one of the fundamental properties as it also provides a measure of the galaxy formation and and evolution. The bimodal distribution of galaxies in the color-magnitude diagram that place them in the red sequence and blue cloud not only reflects the Hubble type, but also the dependence of the distribution on the galaxy stellar mass. Sorting galaxies by $M_\star$ we can study how their properties scale among the different classes. With CALIFA, thanks to the spatial information, we can check how important are the local ($\mu_\star$- driven) and global ($M_\star$-driven) processes in determining the star formation history and chemical enrichment in galaxies.

We find that there is a strong relation between the local values of $\mu_\star$ and the metallicity which is similar in amplitude to the global mass metallicity relation that exits between $\langle \log Z/Z_\odot \rangle_M$ and $M_\star$ over the whole 10^9 to 10^{12} $M_\odot$ range (González Delgado *et al.* 2014b). This means that local and global processes are important in the metallicity enrichment of the galaxies. However, the balance between local and global effects varies with the location within a galaxy. While in disks, $\mu_\star$ regulate the stellar metallicity, producing a correlation between log $\mu_\star$ and $\langle \log Z/Z_\odot \rangle_M$, in bulges and ellipticals is $M_\star$ who dominates the chemical enrichment (Fig.4). Furthermore, in spheroids the chemical enrichment happened much faster and earlier than in disks.

These results are in agreement with the analysis of the star formation history of galaxies (González Delgado *et al.* 2014a). We have shown that mean stellar ages (a first moment descriptor of the SFH) relate strongly to $\mu_\star$ in galactic disks, indicating that local properties dictate the pace of star-formation. The slower growth (hence younger ages) found at low $\mu_\star$ should lead to less metal enrichment, in agreement with the μZR realtion. Within bulges/spheroids, $M_\star$ is a much more relevant driver of the SFH. Most of the star formation activity in these regions was over long ago, leading to fast metal enrichment and little or no chemical evolution since those early days.

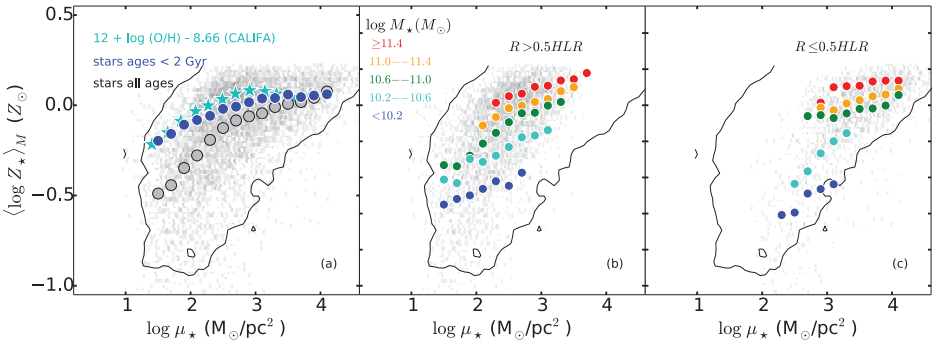

Figure 4. Left: Local stellar metallicity versus the local stellar mass surface density. The grey circles tracks the $\mu_\star$-binned stellar metallicity relation (μZR). Blue circles show the μZR obtained considering only star younger than 2 Gyr in the computation of the metallicity. Cyan stars show the CALIFA-based nebular μZR of Sánchez *et al.*(2013). Middle and right: The mean μZR obtained by breaking the 300 galaxies sample into five M$_\star$ intervals, restricting the analysis to spatial regions outwards and for the inner R= 0.5 HLR

Acknowledgements

This contribution is based on data obtained by the CALIFA survey (http://califa.caha.es), funded by the Spanish MINECO grants ICTS-2009-10, AYA2010-15081, and the CAHA operated jointly by the Max-Planck IfA and the IAA (CSIC). The CALIFA Collaboration thanks the CAHA staff for the dedication to this project. Support from CNPq (Brazil) through Programa Ciência sem Fronteiras (401452/2012-3) is duly acknowledged.

References

Blanton, M. R. & Moustakas, J. 2009, *ARAA*, 47, 159
Bundy, K., *et al.* 2014, https://www.sdss3.org/future/manga.php
Bruzual G., Charlot S. 2003, *MNRAS*, 344, 1000
Cappellari, M, Emsellem, E., *et al.*, 2011, *MNRAS*, 413, 813
Cid Fernandes, R., Mateus, A., Sodré, L., *et al.* 2005, *MNRAS*, 358, 363
Cid Fernandes, R., Pérez, E., García Benito, R., *et al.* 2013, *A&A*, 557, 86
Cid Fernandes, R., González Delgado, R. M., Pérez, E., *et al.* 2014, *A&A*, 561, 130
Croom, S., Lawrence, J. S., Bland-Hawthorn, J., *et al.*, 2012, *MNRAS*, 421, 872
García-Benito, R., *et al.*, 2014, *A&A*, submitted
González Delgado, R. M., Cerviño, M., Martins, *et al.* 2005, *MNRAS*, 357, 945
González Delgado, R. M., Pérez, E., Cid Fernandes, R., *et al.* 2014a, *A&A*, 562, 47
González Delgado, R. M., Cid Fernandes, R., García-Benito, R., *et al.* 2014b, *ApJ*, 791, L16
Husemann, B., Jahnke, K., Sánchez, S. F., *et al.* 2013, *A&A*, 549, A87
Pérez, E., Cid Fernandes, R., González Delgado, R. M., *et al.* 2013, *ApJ*, 764, 1L
Roberts, M. S. & Haynes, M. P., *ARAA*, 32, 115
Sánchez, S. F., Kennicutt, R. C., Gil de Paz, A., *et al.* 2012, *A&A*, 538, 8
Sánchez, S. F., Rosales-Ortega, F. F., Jungwiert, B., *et al.* 2013, *A&A*, 554, 58
Vazdekis, A., Sánchez-Blázquez, P., Falcón-Barroso, J., *et al.* 2010, *MNRAS*, 404, 1639
Walcher, C. J. , Wisotzki, L., Bekeraité, S., *et al.* 2014, *A&A*, arXiv1407.2939